Effects of restrained thermal strains in transversal direction of concrete slab frame bridges

Abbas Zangeneh Kamali, Christoffer Svedholm,
Morgan Johansson
Stockholm, Sweden 2013

Effects of restrained thermal strains in transversal direction of concrete slab frame bridges

Coordinators: Costin Pacoste, Mario Plos

Contributors

Abbas Zangeneh Kamali	KTH, ELU Konsult	Chapters 1-8, Appendix A,B
Christoffer Svedholm	KTH, ELU Konsult	Chapters 1-8
Morgan Johansson	Reinertsen	Chapters 2.3, 7.1

Reference group

Ebbe Rosell (Trafikverket), Mario Plos (Chalmers), Morgan Johansson (Reinertsen), Costin Pacoste (ELU Konsult)

Foreword

In the last few years the usage of 3D finite element analyses has increased substantially in the bridge design community. Such analyses provide the possibility for a more accurate study of the structure than what is possible by using more traditional design tools. However, in order to use the full strength of the finite element method in daily design practice a number of critical issues have to be addressed. These issues are related either to the FE-modelling itself (geometry, support conditions, mesh density, etc.) or to the post processing of the obtained results (stress concentrations, choice of critical sections, distribution widths and so on). In the latter category, one problem of special significance refers to concrete structures subjected to restrained forces caused by temperature loading or shrinkage.

In this context, the present report addresses the problem of crack width control in transversal direction for concrete slab frame bridges subjected to restrained thermal or shrinkage loading. The recommendations given herein are based not only on the existing literature but also on the authors own investigations using non-linear finite element analyses.

The authors want to express their gratitude to the members of the reference group. Their comments and suggestions have been invaluable in shaping the report.

Contents

List of Abbreviations

2D: Two Dimensional

3D: Three Dimensional

ACI: American Concrete Institute

EC: Eurocode

FE: Finite Element

FEM: Finite Element Method

ICE: Institution of Civil Engineers

List of Notations

α_T	Thermal expansion coefficient
A_w	Cross section area of concrete wall
A_f	Cross section area of foundation slab
c	Concrete cover
c_k	Creep factor
E_w	Elastic modulus of concrete wall
E_f	Elastic modulus of concrete foundation slab
E_{cm}	Mean elastic modulus of concrete
E_s	Characteristic modulus of elasticity for steel
ε	Strain
ε_c	Compressive strain in concrete
ε_{c1}	Compressive strain at peak compressive stress
ε_t	Tensile strain in concrete
ε_{uk}	Ultimate strain in steel
$\varepsilon_{sm} - \varepsilon_{cm}$	Differential strain between concrete and steel
f_{cm}	Mean compressive strength of concrete
f_{ck}	Characteristic compressive strength of concrete
f_{ctm}	Mean tensile strength of concrete
f_{yk}	Characteristic yield strength of steel
f_{uk}	Characteristic ultimate strength of steel

ϕ	Diameter of reinforcement bar
φ_c	Creep coefficient
G_f	Fracture energy of concrete
h	Distance from restrained edge
h_{wm}	Distance from restrained edge to maximum crack width
H	Height of the wall
k	Factor which consider the effect of non-uniform self-equilibrating stresses
k_1	Factor which considers the bond properties of reinforcement
k_2	Factor which considers the distribution of strain
k_c	Factor consider stress distribution in section immediately prior to cracking
k_t	Factor depending on the duration of the load
L	Length of the wall
l_e	Element length
N_x	Axial force in transversal direction
ρ_s	Reinforcement ratio
ρ_{eff}	Effective reinforcement ratio
R	Restraint degree
$S_{r,max}$	Maximum crack spacing
$S_{r,avg}$	Averaged crack spacing
t	Thickness of the wall
ΔT	Temperature difference
ΔT_T	Temperature difference due to thermal differences
ΔT_S	Temperature difference due to shrinkage
w_{max}	Maximum crack width
w	Crack width
σ_s	Stress in reinforcing steel
σ_c	Compressive stress in concrete
σ_t	Tensile stress in concrete
σ	Stress
ν	Poisson ratio

1. Introduction

Nowadays, 3D linear FE models are widely used for the analysis of concrete structures with complex geometries. Although successful in many respects, these models have certain drawbacks. One of these drawbacks is apparent when the structure is subjected to restrained forces caused by temperature loading or shrinkage. The problem in this context is that a linear model will predict very large restraint forces. If these forces are used in the design, for instance for crack width controls (see for instance section 7.3.4 of EC2-2 (2005)), this will (incorrectly) result in very large amounts of reinforcement. One typical example of such a situation is that of a concrete wall cast against an existing concrete foundation or concrete slab. Since the shrinkage in the two members will be different, the foundation (or the slab) will restrain the free deformation of the wall thus inducing restraint forces in the structure. A similar situation occurs if the concrete wall and the slab are subjected to different temperature variations with one of the elements restraining the free deformations of the other. Due to this restraining action, a linear FE model will predict large tensile forces in the transversal direction of the wall or the slab. In reality however, due to the cracking of concrete the restraint forces will be considerably reduced. Unfortunately linear elastic models cannot capture this behaviour.

It is well-known that the restraining forces are different in nature from forces caused by other types of external loading, such as for instance gravity or traffic and thus their effect should be studied in a different manner. However, the design procedures in chapter 7 of EC2-2 (2005) offer very little guidance on how to address the issue of restraint forces in the context of crack width control. During the last 10-15 years several numerical and analytical investigations have been performed with the aim of understanding in some detail the behaviour of concrete structures subjected to restrained thermal strains – see for instance Pettersson and Thelandersson (2001), Andersson and Andersson (2010), Alfredsson and Spåls (2008), Johansson and Lantz (2009) and Antona and Johansson (2011), to cite just some of the work performed in Sweden. Based on this type of numerical and analytical studies but also to a large extent on experimental investigations, ACI (1995), Kheder (1998) and EC2-3 (2006) proposed some simplified methods and recommendations for describing the behaviour of reinforced concrete members subjected to restrained thermal strains and for estimating the crack spacing and the crack width.

1.1. Aim and scope

The main aim of this report is to propose an efficient methodology for dealing with the restraint forces induced by thermal or shrinkage loading in the context of the serviceability limit state requirements as formulated in EC2. For this purpose several simplified methods presented in the literature for crack width controls have been considered. The estimations based on these simplified methods have then been compared with the results obtained from non-linear FE analyses.

1.2. Limitations

In this report, only the effect of short term restrained thermal strains on the structure has been studied. The effects of shrinkage and early age thermal cracking including creep or any other types of external loads have not been included in the analysis.

Only the uniform temperature difference between different structural parts of a slab frame bridge was considered. Other thermal load cases which do not cause significant restraint forces (especially in transversal direction) were neglected. A uniform constant temperature was applied to each structural part without any detailed thermal analysis.

1.3.   Outline of the report

A theoretical background for the subject is presented in chapter 2. It includes a short introduction to thermal actions on bridges and it also describes the problems related to restrained thermal strains in 3D linear FE models. The crack control design procedure according to EC2 is also presented together with some experimental investigations in this field.

Chapter 3 presents a brief description of the case studies used in this report. For these case studies, the results obtained using the simplified design procedures presented in EC2-3 are presented in Chapter 4.

In chapter 5 and 6, the input values, method and results of the linear and non-linear FE analysis of the case studies are presented.

Chapter 7 contains a comparison between the results obtained using the simplified procedure and the FE results, followed by the main conclusions of the study. Based on these conclusions, practical recommendations are presented in Chapter 8 together with some suggestions concerning future studies.

2.   Theoretical background

2.1.   Thermal actions on bridges based on EC2

According to EC2-1-1 (2004), thermal effects should be taken into account only when checking the serviceability limit states, except for some special cases such as fatigue conditions or verification of stability where second order effects are important.

Thus, according to EC1-1-5 (2003), different thermal actions should be applied on bridge structures to check their serviceability limit states. Since this report focuses on the effects of temperature changes in the transversal direction of slab frame bridges, only the temperature difference load case corresponding to section 6.1.6 in EC1-1-5 (2003) is investigated.

According to the provisions in the code, a uniform temperature difference of 15°C should be applied between the main structural components of the bridge (e.g. deck and wall of a slab frame bridge), see figure 2.1.
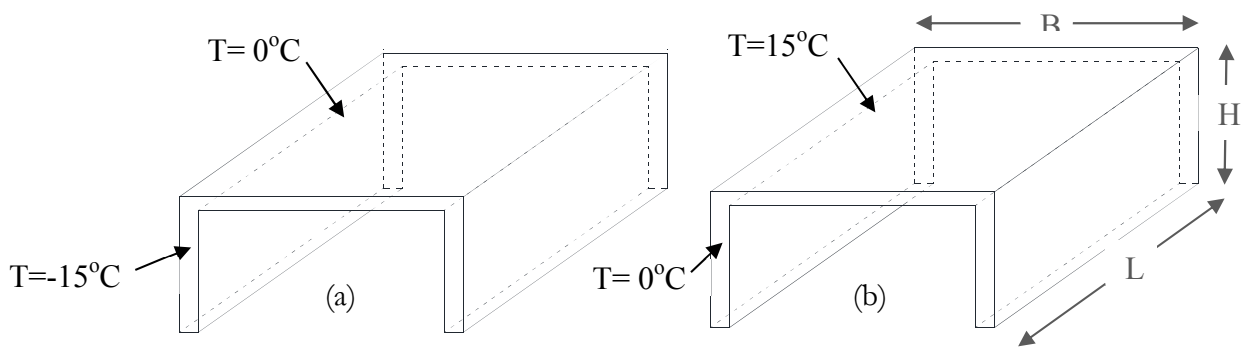

Figure 2.1 Temperature difference between deck and wall in slab frame bridges

2.2.   Analysis using 3D linear FE models

Before the development of finite element commercial analysis tools, 2D frame models were commonly used to analyse and design slab frame bridges. In such a 2D frame model, the effect of temperature differences and/or shrinkage is only considered in the longitudinal direction and is totally ignored in the transversal direction. In order to consider the 3D effects for different actions especially for skewed bridges, 3D FE models have been used in recent years in the current design practice. However, if such linear models are used, applying a temperature difference between the deck and the wall of the bridge (see figure 2.1) will result in very large normal forces in transversal direction (see figure 2.2). Using these forces in the usual crack control procedures leads to extremely large reinforcement ratios which are neither realistic nor practical. In reality, the restraint forces will be reduced to a very large extent as the stiffness of the structure is decreased during cracking and this behaviour cannot be represented by linear elastic models.
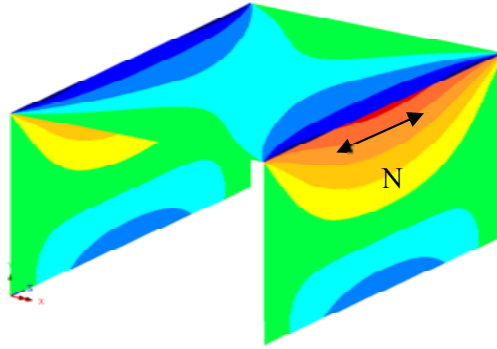
Figure 2.2. Restrained forces in the transversal direction of the bridge due to temperature differences

One conclusion of the above discussion is that the linear elastic sectional forces which are due to the restraint actions should be treated differently from the forces caused by other types of external loading. In this particular case, it can be stated that considering the nonlinear behaviour of reinforced concrete and its stiffness degradation as a result of cracking is essential for a rational design. In current design practice however, it is very difficult to use non-linear models. Bridge structures are usually designed for a wide range of loads, including moving traffic loads placed in various settings aimed at generating the most adverse effects at relevant locations. In these settings a non-linear analysis becomes quickly prohibitive since the superposition principle cannot be utilised. Moreover, due to unsolved uncertainties concerning the safety format, non-linear FE-analyses are at present not allowed for bridge design according to the Swedish national annex (NA) to EN 1992.

2.3.   Restraint forces

Restrained forces differ fundamentally from external (applied) loads. The external loads are loads applied to the boundaries of a structure, such as gravity or traffic loads. On the other hand, the restraint forces are generated when a structure is prevented from movement relative to its unloaded shape, i.e. due to uneven support settlements, temperature differences or shrinkage between adjacent structural parts. The restraint forces are thus directly linked to the structural stiffness properties and by consequence reduced when the stiffness decreases, Cope (1984) and Engström (2011).

Engström (2011) and Ghali et al. (2002) state that in the case of external loading, directly after crack formation, the load remains equal to the cracking load and it then increase gradually until the member reaches the 'stabilized cracking stage' as shown in Figure 2.3. On the other hand, in the case of restraint loading, during crack formation, the load instead decreases suddenly due to the decrease of overall stiffness and the stabilized cracking stage rarely occurs. This difference in response of a reinforced concrete member subjected to external and restraint loading is schematically illustrated in Figure 2.4. Since the restraint forces depend on the structural stiffness, there is no apparent 'known' force to design the reinforcement for, Engström (2011). Consequently, in the case of restraint loading, the crack width control and reinforcement design cannot be done in the same way as for other types of external loads.
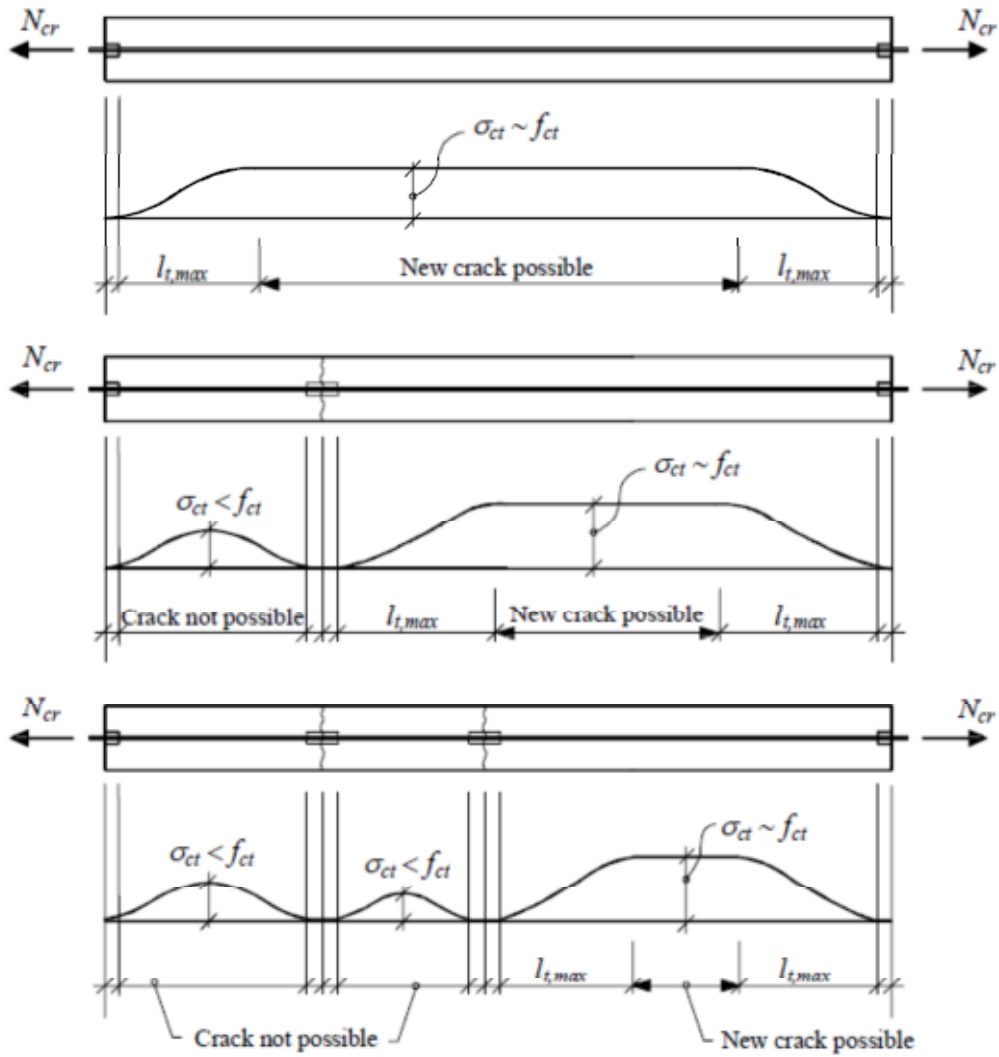
Figure 2.3. Cracking process of a reinforced concrete member. When the distance between the cracks become small enough no more cracks may form and stabilized cracking is reached. From Engström (2011).

F F

u

F F

u u

(a)   (b)
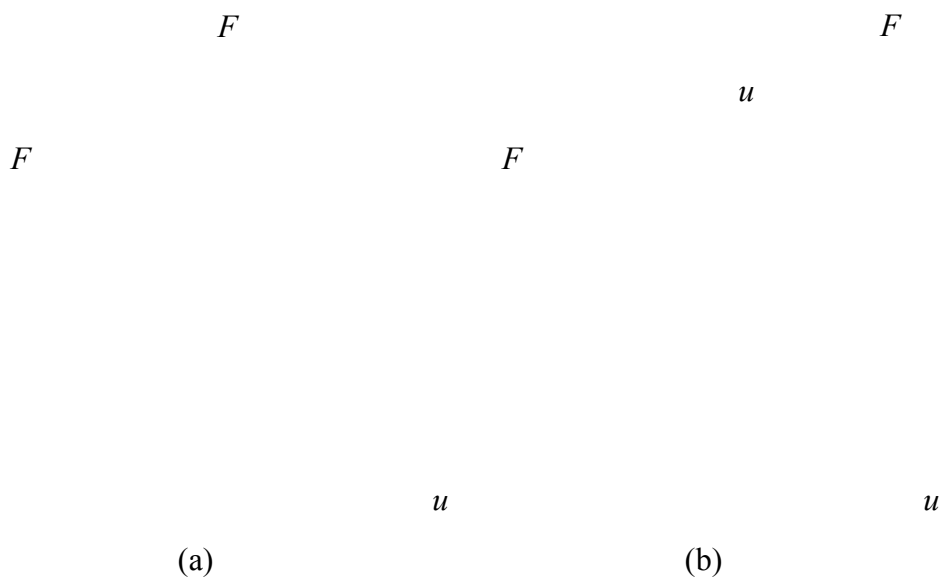
Figure 2.4. Response of a reinforced concrete memer subjected to (a) external load and (b) restrained load. From Alfredsson and Spåls (2007).

For more information about the concepts of restraint forces and detailed description of cracking process in the case of restraint loading, see Engström (2011) and Ghali et al. (2002).

2.3.1.   Restraint cases

There are different types of restraint cases which partially or fully prevent the free deformation of the structure. Two of these, shown in figure 2.5 have been extensively studied by several researchers, Kheder (1997), Engström (2011), Bamforth et al. (2010), Johansson and Lantz (2009), Antona and Johansson (2011).

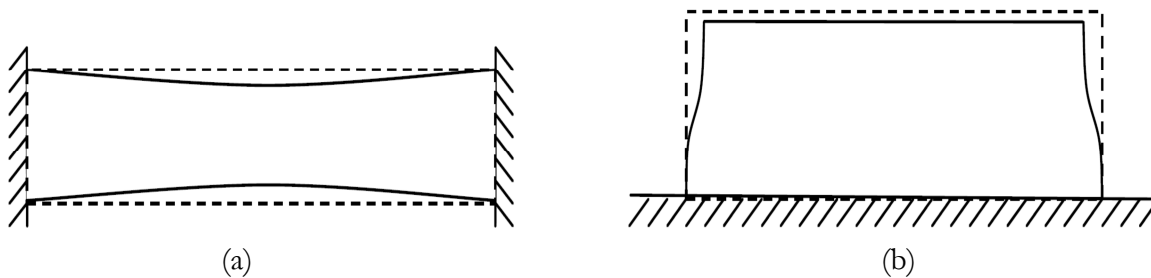*Figure 2.5. Different restraint cases. (a) restraint of a member at its ends; (b) continuous restraint along one edge*

In current design practice, complex structures are often simplified and reduced to one of these two restraint cases. For example, the restraint condition between the deck and wall of a slab frame bridge can be simplified to a wall continuously restrained along one of its edge, see figure 2.1(b). This report especially treats case (b) with continuous edge restraints.

2.3.2.   Restraint degree

The restraint degree *R*, quantifies the extent to which a structural member is prevented from moving freely relative to its boundaries. If the edge restraint is fully rigid, no movement is allowed and there is a full restraint condition with *R=1*. If however the support has some flexibility, the restraint degree R will be lower than 1.

For a wall cast against a slab and continuously restraint along one edge, ACI (1995) proposed a method for estimating the reduction of the restraint degree based on the relative axial stiffness of the connected members:

$$R_{edge} = c_k / (1 + \frac{A_w}{A_f} \frac{E_w}{E_f})$$

(2.1)

The coefficient c_k in eq. (2.1), is introduced to consider the effect of creep in the case of sustained loading. In EC2, the creep coefficient is assumed as constant, i.e. c_k = *0.65* (Bamforth et al, 2010).

The value of the restraint degree is strongly dependent on the stiffness ratio of the connected members and the duration of the loading. Table 2.1 presents different edge restraint degrees calculated based on the eq. (2.1) for different cases.

Table 2.1. Edge restraint degree for different cases

Case	c_k	A_f/A_w [*]	E_w/E_f	R_{edge}
Stiff foundation slab[*]- Long term loading	0.65	2.5	1	0.47
Stiff foundation slab[*]- Short term loading	1	2.5	1	0.72
Fully rigid foundation slab - Short term loading	1	∞	1	1

* The maximum effective restraining slab foundation area A_f, can be assumed as equal to 2.5 times the wall area A_w, (ACI ,1995)

The value of the restraint degree calculated by eq. (2.1) is the value at the intersection between the wall and the foundation slab. Depending on the wall geometry, in particular the length/height ratio of the wall, the restraint coefficient will decrease with the distance from the intersection to varying degrees, as shown in figure 2.6. Thus, the upper part of the wall is almost free to move while the areas close to the fixed edge are much closer to a fully restrained condition.
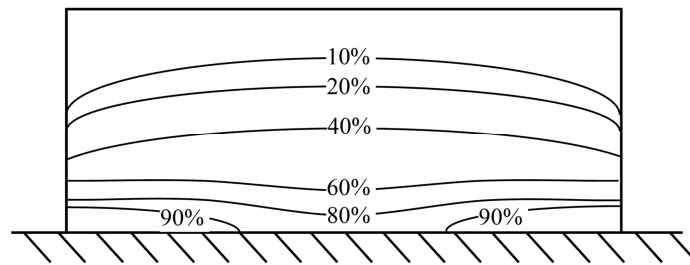
Figure 2.6. Example of variation of restraint degree in members with continuous base restraint, Concrete handbook material (1994) - (Assumed $R_{edge} = 1$)

In order to quantify these effects, Betonghandboken Material (1994) proposed a series of curves describing the variation of the restraint degree along the height of the wall at mid-section for different L/H ratios (see figure 2.7). Based on the values in figure 2.5, for walls with L/H ratio greater or equal to 7 almost the whole mid-section of the wall is fully restrained against movement.
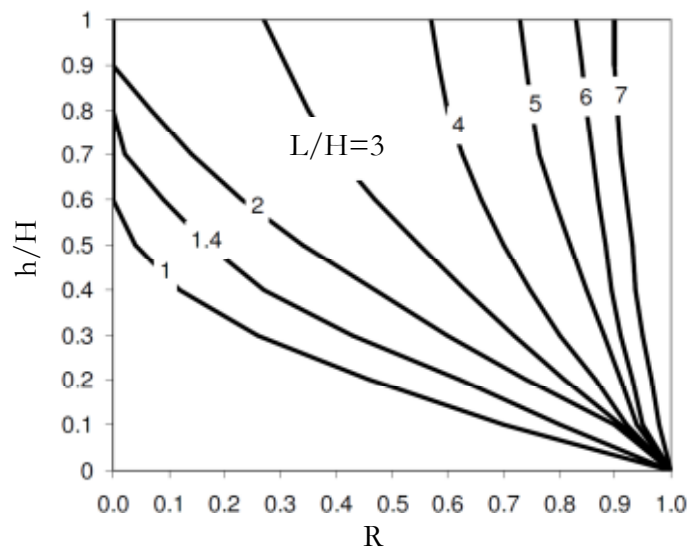

Figure 2.7. Variation of the restraint degree along the height of the wall at mid-section Betonghandboken Material (1994) - (Assumed $R_{edge} = 1$)

2.4. Design for crack control according to EC2

2.4.1. Maximum allowable crack widths (w_{max})

If the crack widths calculated in accordance with the models given in EC2 are limited to the values given in table 7.101N of EC2-2 (2005), the performance of the bridge structure is unlikely to be impaired. The values of the maximum allowable crack width are dependent on the exposure class. Without any loss of generality, for the purposes of this section it will be assumed that the maximum allowable crack width is equal to *0.3mm*, i.e the maximum crack width should be smaller than *0.3mm* for reinforced concrete members under quasi-permanent load combination.

2.4.2. Minimum reinforcement in sections subjected to tension

According to section 7.3.2 of EC2-2 (2005), a minimum amount of bonded reinforcement is required to control cracking in areas where tension is expected. The amount may be estimated from equilibrium between the tensile force in concrete just before cracking and the tensile force in reinforcement at yielding (see eq. (2.2)). According to section 9.6.3 of EC2-2 (2005), the total horizontal reinforcement ratio running along the length of the wall should not be less than 0.2%.

$$\rho_{s,min} = \frac{k.k_c.f_{ctm}}{f_{yk}} \geq 0.2\% \tag{2.2}$$

For bridge structures, f_{ctm} in equation 2.2 should be greater than 2.9MPa in order to cater for shrinkage, see EC2-2 (2005).

2.4.3. Crack calculation according to EC2-2

According to section 7.3.4 of EC2-2 (2005), at sections where the minimum reinforcement according to section 2.4.2 is provided, the design crack width can be calculated as follows:

$$w_k = S_{r,max}(\varepsilon_{sm} - \varepsilon_{cm}) \tag{2.3}$$

$$S_{r,max} = 3.4c + \frac{0.425k_1\ k_2\ \phi}{\rho_{eff}} \tag{2.4}$$

$$\varepsilon_{sm} - \varepsilon_{cm} = \frac{\sigma_s - k_t \dfrac{f_{ctm}}{\rho_{eff}}(1 + \dfrac{E_s}{E_{cm}}\rho_{eff})}{E_s} \geq 0.6\frac{\sigma_s}{E_s} \tag{2.5}$$

Note that equations (2.4) and (2.5), which gives the maximum crack distance and differential strain between concrete and steel, respectively, are applicable for cases where a stabilized cracking stage has been reached under external loading. Based on the definitions in the code, the stress in the reinforcement (σ_s) is calculated based on a cracked section. The main assumption in this context is that the section forces still exist and are not reduced after cracking. For this reason equation (2.4) is only applicable if a stabilized cracking is reached and equation (2.5) is not applicable at all in case of restraint loading, see section 2.3.

2.4.4. Crack calculation according to EC2-3

According to section M.3 in EC2-3 (2006), in the case of a long wall restrained along one edge and subjected to thermal or shrinkage strains, if the minimum reinforcement given in section 2.4.2 is provided, the design crack width can be estimated by eq. (2.3) in the same way as described in EC2-2 (2005), but the expression $(\varepsilon_{sm} - \varepsilon_{cm})$ in eq. (2.5) should be replaced by eq. (2.6).

$$\varepsilon_{sm} - \varepsilon_{cm} = R\,(\alpha_T.\Delta T), \tag{2.6}$$

where R is the restraint factor taking into account the effect of the edge restraint. According to table 2.2, the maximum suggested restraint degree is equal to $R=0.5$. This value is for long term thermal/shrinkage loading case including the creep effects (Bamforth et al. 2010).

Table 2.2. Restraint factors for the central zone of walls (EC2-3, 2006)

L/H	R at restrained edge	R at free edge
< 2	0.5	0.0
3	0.5	0.05
4	0.5	0.3
> 7	0.5	0.5

Note also that the recommended value for R according to table 2.1 is more conservative (i.e. $R=0.72$) since that value is for short-term temperature loading and does not include the effect of creep. For more information about the restraint degree see section 2.3.2.

2.4.5. Control of cracking without direct calculations

According to section 7.3.3 in EC2-2 (2005), for sections in tension caused dominantly by restraint, if the minimum reinforcement according to section 2.4.2 is provided, crack widths are not likely to be excessive if the maximum bar size is limited to the values given in figure 2.8.

For cracking caused dominantly by restraint, the steel stress is the value obtained immediately after cracking (i.e. σ_s in expression 2.7)

$$\sigma_s = \frac{k\,k_c\,f_{ctm}}{\rho_s} \qquad (\rho_s \geq \rho_{s,\min}) \tag{2.7}$$
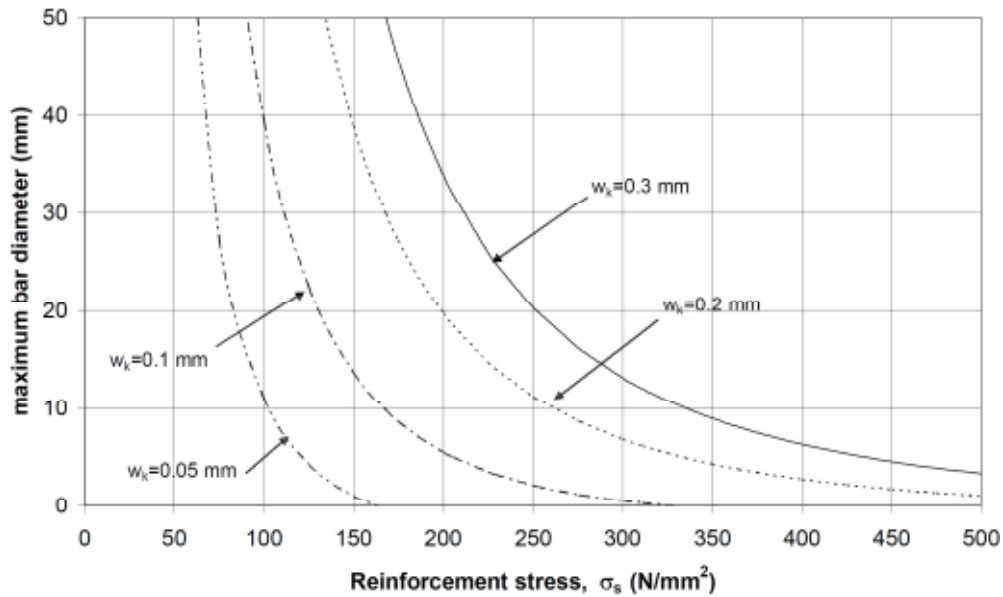
Figure 2.8. Maximum bar diameter for crack control in members subjected to axial tension (EC2-3, 2006)

2.4.6. Provision of construction joints

According to Annex N in EC2-3 (2006), there are two main options for dealing with restraint forces in concrete structures:

(a) Design for free movement. Close movement joints must be provided at spacing less than $\max(5m, 1.5H)$ where H is the wall's height in meters. Hence, cracking is controlled by the proximity of joints and significant cracking between the joints may not occur. In this case providing the minimum reinforcement according to section 9.6.3 in EC2-2 (2006) is sufficient.

(b) Design for full restraint. In this case, no joints allowing movement are provided and the crack widths and spacing are controlled by the provision of appropriate reinforcement according to the sections 2.4.4 and 2.4.5.

2.5. Some points from experimental investigations

The results obtained from experimental investigations in this field can be used as reference points for better understanding the nature of the problem and for the verification and calibration of the numerical models.

The results of experimental investigations on base restrained walls subjected to long-term shrinkage/thermal strains (see Kheder (1997)), indicate a typical pattern for the cracking behaviour of this type of structures. Thus, figure 2.9 shows the typical observed crack pattern in a base restrained wall. The primary cracks occur in the middle of the wall followed by some inclined cracks at the corners.
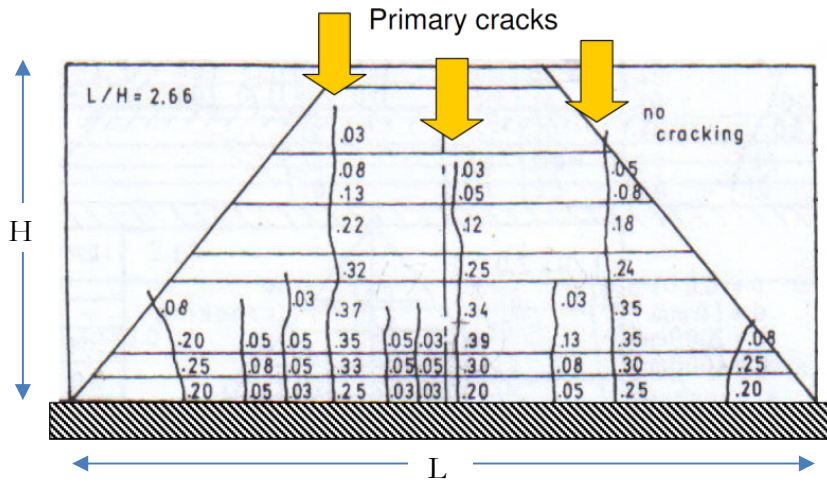
Figure 2.9. Typical observed crack pattern in a base restrained wall (Kheder, 1997)

Reported crack width data by Kheder (1997) suggests that the maximum crack width is likely to occur above the restrained edge at a height which is about 10% of the wall's length. According to ACI (1995), the maximum crack width usually occurs at heights of about 10-15% of the wall length measured from the restrained edge, see figure 2.10.
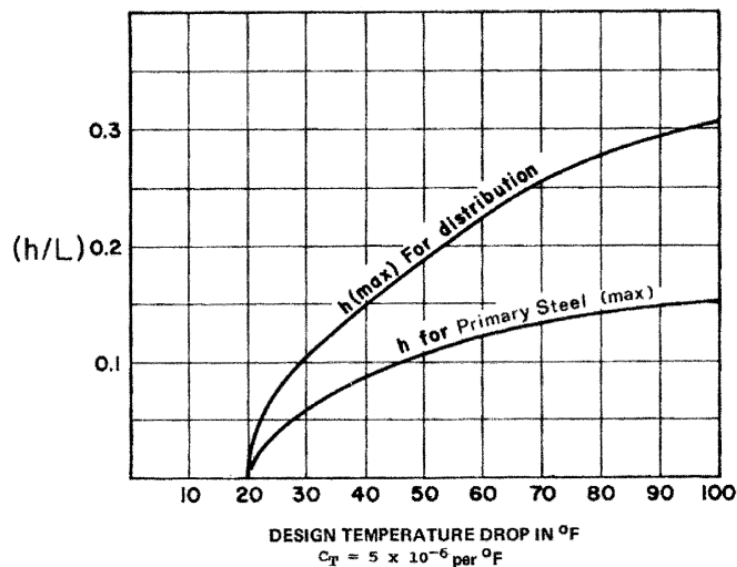
Figure 2.10. Location of the maximum crack width (ACI (1995))

2.6. Comments on the EC2-3

Bamforth et al. (2010) carried out a comprehensive study concerning the crack width computation procedure presented in EC2-3 (2006), see also section 2.4.4. The main conclusions of this work are summarised below:

- The effect of the wall geometry on the crack spacing is not considered
- The stress in the steel after cracking is not taken into account.
- The tensile strength of concrete does not play any role.

- The positive effects from edge restraint which decreases the crack width are neglected. Since part of the load from the concrete is transferred into the restraining edge, the higher edge restraint will reduce the crack spacing, hence crack width will also decreased.
- **The provided minimum reinforcement ratio in this procedure is conservative.**

Figure 2.11.Comparison of measured crack widths by Kheder(1997) and estimated crack widths based on EC2-3

A comparison between measured crack widths (see Kheder (1997)) and crack widths estimated using the method in EC2-3, is presented in figure 2.11. As can be seen, the EC2-3 method gives higher estimates of crack widths for 90% of the samples and can thus be considered to be conservative.
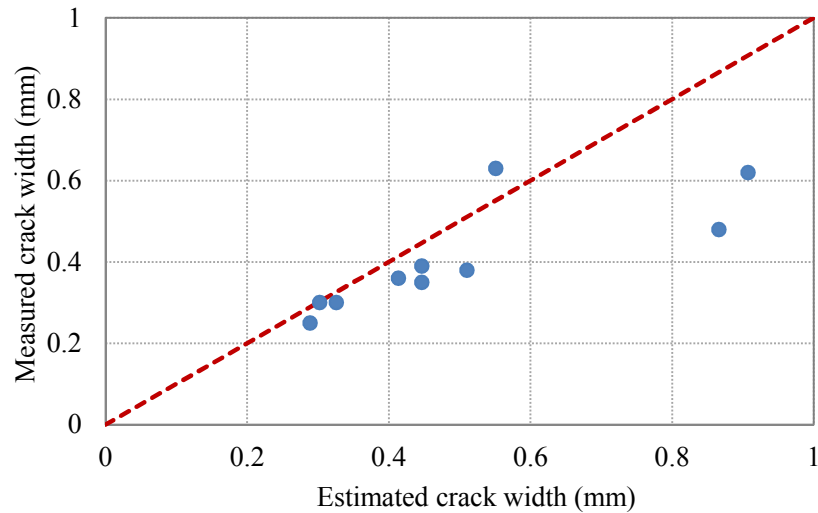
3.   Test cases

This chapter describes the dimensions and properties of the structural configurations used to investigate the cracking behavior of the wall of a slab frame bridge subjected to restrained thermal strains. The investigation includes both linear and non-linear FE analyses, which are further compared with the results obtained using different code approaches.

3.1.   Geometry and boundary conditions

In order to simplify the analysis, a 2D model of the bridge's wall was used (see figure 3.1). Furthermore, due to symmetry, only half of the wall was considered. The deck at the top of the wall was assumed as infinitely rigid (along the wall) which is conservative. It was also assumed that the bottom plate and the wall were cast together and that there was no temperature difference between them. Hence the bottom edge was assumed as fully unrestrained along the wall.
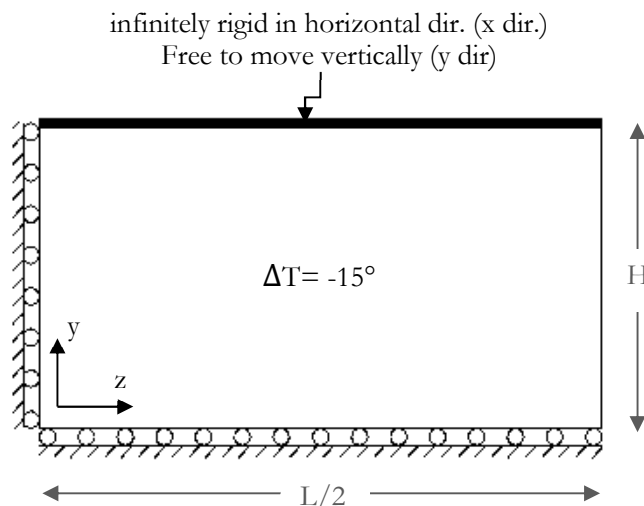
Figure 3.1. General configuration and boundary conditions of the 2D FE model

In order to investigate the effect of the L/H ratio on the results, models with different L/H ratio were studied (see Table 3.1).

Table 3.1. Dimensions of the models

H (m)	t (m)	L (m)	L/H
		3	1
		6	2
3.0	0.5	9	3
		12	4
		21	7

3.2. Loading

The whole region of the wall is subjected to a uniform temperature decrease equal to -15°C, see figure 3.1.

3.3. Material properties

The material properties of concrete and reinforcing steel which were used in the linear and non-linear FE analysis and also in the design code calculations are presented in table 3.1.

Table 3.1. Material properties used in analysis and design EC2-1-1 (2004), MC2010 (2010)

Concrete C30/37			Reinforcing steel		
	Linear	Non-linear		Linear	Non-linear
f_{cm} (MPa)	–	38	f_{yk} (MPa)	–	500
f_{ctm} (MPa)	–	2.9	f_{uk} (MPa)	–	600
E_{cm} (GPa)	32	32	E_{sk} (GPa)	–	205
ε_{c1} (%)	–	0.21	ε_{uk} (%)	–	7.5
ν	$0^{(1)}$	$0.2^{(2)}$			
G_f (N/m)	–	140			
α_T (°C^{-1})	10^{-5}	10^{-5}			

(1) Cracked section   (2) Uncracked section

4. Crack calculation based on EC2-3

The approach in EC2-3 (2006) (see also section 2.4.3) for the crack width control of a wall restrained along one edge and subjected to thermal or shrinkage strains was used in this chapter in order to evaluate the crack widths of the previously introduced test cases. These results will further be compared with the values provided by non-linear FE-analyses and also with the method in EC2-2 (2005) combined with a linear FE analysis.

4.1. Method

According to section 2.4.2, minimum reinforcement should be provided for all test cases described in chapter 3. Based on eq. (2.2), for a wall with thickness 0.5m, the minimum reinforcement that should be provided is 0.37% which corresponds to $\phi 12s125mm$ at each face of the wall in transversal direction.

According to EC2-3 (2006), the restraint degree at the joint should be taken as $R=0.5$. However, as mentioned at the end of section 2.4.4 this value is valid for a wall connected to a relatively stiff foundation under long term thermal and/or shrinkage strains thus including the creep effects also. However, in this report, in order to enable a direct comparison with the FE results, the slab foundation is assumed as infinitely rigid and the effect of creep is disregarded. For this reason the restraint degree is instead assumed to be $R=1$ (see also table 2.1).

4.2. Results of code calculations

Table 4.1 presents the input values and results of the crack width calculation based on the approach in EC2-3 (2006). The calculated maximum crack width for all test cases is equal to 0.15mm.

Table 4.1. Crack width calculation based on EC2-3

c (mm)	ϕ (mm)	ρ_s (%)	ρ_{eff} (%)	k_1k_2 (-)	$S_{r,max}$ (m)	R_{edge} (-)	α_T (°C⁻¹)	ΔT (°C)	$\varepsilon_{sm} - \varepsilon_{cm}$ (-)	w_{max} (mm)
75	12	0.37	0.55	0.8	1	1	10^{-5}	15	0.00015	0.15

5. Linear FE analysis

5.1. Introduction

The purpose of this chapter is to investigate the magnitude of the restraint forces as given by a linear elastic FE analysis for the test cases defined in chapter 3. These restraint forces are then used to design the reinforcement based on the standard crack width control method in EC2-2 (2005).

5.2. Method

The general purpose commercial finite element software, Abaqus/Implicit version 6.11 (Hibbitt et al. 2011) was used to model and analyze the wall. A 2D plane stress FE-model was created based on the geometry in figure 3.1.

As the temperature load is a simple uniform temperature change which applies to the whole model, the analysis type was made as a structural analysis and no heat flow had to be performed. The temperature drop is introduced as a predefined field and applied in one single step.

5.3. Finite element mesh

The wall was represented by 4-node bilinear plane stress finite elements (CPS4) with a full integration scheme. The FE mesh was uniform with an element size of 5 by 5 cm. The size of the elements was selected based on a convergence study (for details see appendix A).

5.4. Results of the linear FE analyses

Figure 5.1 (a)-(e) present contours of the tensile forces in the transversal direction of the wall for different L/H ratios. As can be seen from the figure, the maximum force value is the same in all cases but the distribution of the tensile force is different. By increasing the L/H ratio, larger parts of the wall cross section are subjected to large tensile forces, which is in good agreement with section 2.3.2, figure 2.4. Table 5.1 summarizes the results of the linear FE analysis. One important observation in this context is that for high L/H ratios the whole section is subjected to a uniform tensile force in the transversal direction.
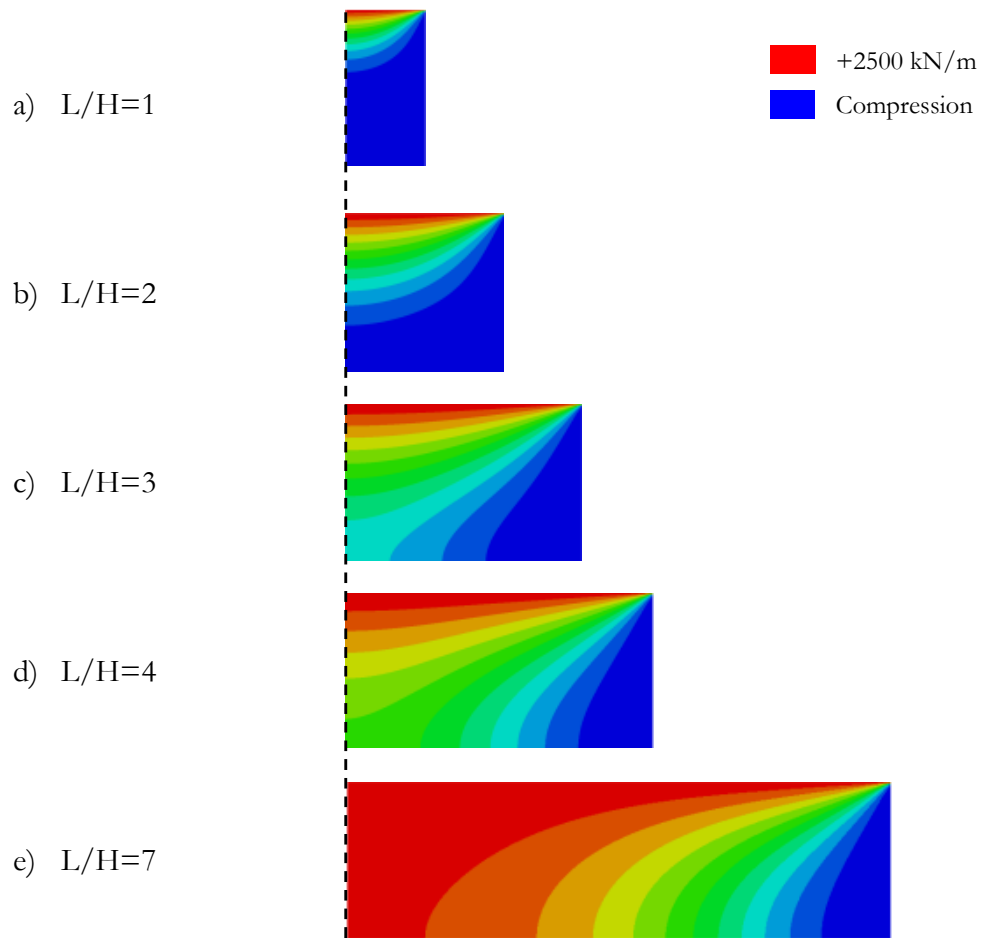
Figure 5.1 (a)-(e). Contours of the restrained horizontal tensile forces in transversal direction of the wall (from linear FE analysis)

Table 5.1. Tensile forces at the symmetry section in transversal direction obtained from linear FE analyses

L (m)	L/H	$N_{x,max}$ (kN/m)	$N_{x,averaged}$ 1m strip at the top (kN/m)	$N_{x,averaged}$ over the height H (kN/m)
3	1	2500	1400	600
6	2	2500	1800	1000
9	3	2500	2050	1400
12	4	2500	2200	1800
21	7	2500	2500	2500

5.5. Crack control based on linear FE analysis & EC2-2

As it was mentioned in section 2.4.3, in the case of restraint loading, the standard crack width control according to EC2-2 combined with the results of a linear FE analysis is not an applicable design procedure as it leads to very large amounts of reinforcement. For the studied test cases, the results of such a procedure are summarized in tables 5.2 and 5.3.

Table 5.2 presents the maximum crack widths evaluated using the restraint forces in table 5.1 (i.e. $N_{x,averaged}$ over a 1m strip at the top) and equations (2.4)-(2.6) for walls with minimum reinforcement ratio.

Table 5.2. Crack width calculation based on EC2-2 and a linear FE analysis (minimum reinforcement ratio)

L (m)	L/H	w_{max} (mm)
3	1	
6	2	
9	3	$> 1.5^{*}$
12	4	
21	7	

* Reinforcing steel yields

Table 5.3 presents the reinforcement required in order to limit the crack width to values smaller than 0.3mm.

Table 5.3. Reinforcement design according to EC2-2 and linear FE analyses, $w_{max} = 0.3mm$

L (m)	L/H	$N_{x,averaged}$ 1m strip at the top		$N_{x,averaged}$ over the height H	
		ρ_s (%)	Reinf. at each face	ρ_s (%)	Reinf. at each face
3	1	1.7	φ20s75	0.9	φ20s150
6	2	2.1	φ25s90	1.3	φ20s100
9	3	2.5	φ25s80	1.7	φ20s85
12	4	2.7	φ28s90	2.1	φ25s90
21	7	3.0	φ28s80	3.0	φ28s80

6. Non-linear FE analysis

The test cases previously introduced have also been analyzed using nonlinear FE models. The modeling assumptions and the results of these analyses are presented in the reminder of this chapter.

6.1. Method

As in the case of the linear analysis, Abaqus/Implicit version 6.11 (Hibbitt et al., 2011) was used to model and analyze the wall. A 2D plane stress FE-model was created based on the geometry in figure 3.1.

As the temperature load is a simple uniform temperature change for the whole model, the analysis type was made as a structural analysis with the temperature drop introduced as a predefined field. To avoid numerical problems, the maximum temperature decrease was limited to 0.015 degree for each analysis step.

The amount of reinforcements plays an important role in such a non-linear FE analysis. Hence, in this analysis both vertical and horizontal reinforcement were modeled. Since the results of the non-linear analysis will be compared to the results obtained from code calculations (see also chapter 4), the same reinforcement ratio will be used (see figure 6.1).
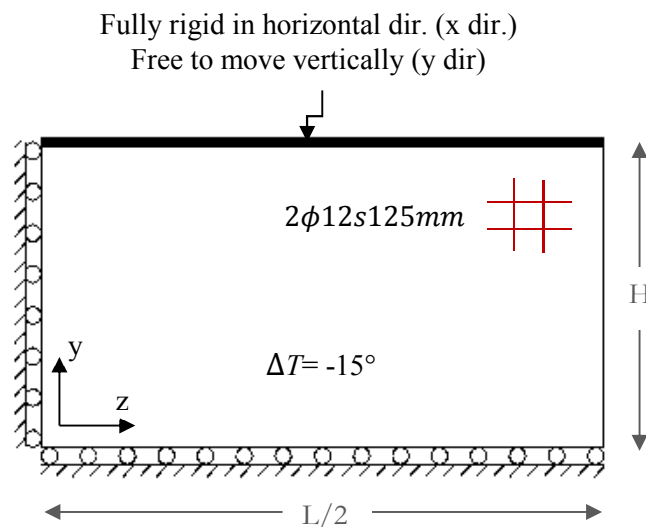

Figure 6.1. General configuration and boundary conditions of the 2D FE model

6.2. Finite element mesh

The whole region was meshed with 4-node bilinear plane stress elements (CPS4) with a full integration scheme. Both horizontal and vertical reinforcements were discretized by 2-node linear truss element (T2D2). The whole model has been discretized with a 5 by 5 cm uniform mesh. The size of elements must be selected small enough to achieve convergence in the results. Details of the mesh size studies performed for this purpose are given in appendix A. Note also that in the case of a nonlinear analysis a finer mesh will also give a better visualization of crack patterns.

6.3.   Material modeling

The material properties of reinforcing steel and concrete used in the non-linear material modeling are presented in table 3.1. To model the non-linear behavior of the concrete the smeared crack material model in Abaqus 6.11 (Hibbitt et al., 2011) was used. For the tensile response after cracking a bi-linear relation according to figure B.1 in appendix B was used. The crack band width i.e. the length over which the crack is smeared, was assumed to be equal to the element length. For the uniaxial compression response of concrete see figure B.2. The non-linear behavior of reinforcing steel is modeled by classical von Mises plasticity, see figure B.3. For more information about the material modeling details and input curves, see Hibbitt et al. (2011). For all other parameters, the default values have been used.

6.4.   Bond behavior

In this analysis, no bond-slip models were included. The interaction between reinforcement and concrete was modelled as fully tied. The connection between the wall and slab deck at the joint was assumed to be fully rigid and no shear-slip relation was used to model the interaction at this interface.

6.5.   Crack pattern and crack width estimation based on non-linear analysis

Figure 6.2 shows the crack patterns in the transversal direction of the wall for different L/H ratios. The contours of total tensile strains are presented in this figure. Table 6.1 presents the maximum values of total concrete strains and estimated maximum crack widths in the transversal direction obtained from the non-linear analysis together with the location of the maximum crack width along the height of the wall. In addition, an estimate of the average crack spacing is also provided. This estimate is based on the distances marked in figure 6.2. These estimates are in reasonably good agreement with the value given by equation (2.4) which is 1m for all considered test cases (see also table 4.1). Note also that, in this report the crack width is calculated by eq. (6.1) based on the value of the total strain in concrete elements and the characteristic element size (the crack band width).

$$w = \varepsilon_t . l_e \tag{6.1}$$

Table 6.1. Crack width estimation based on the non-linear analyses

L (m)	L/H	$max \, \varepsilon_t \, (\times 10^{-3})$	w_{max} (mm)	$s_{r,avg}$(m)	h_{wm}/L (%)
3	1	0.10	0.01	--	7
6	2	1.10	0.06	0.75	8.5
9	3	1.70	0.09	0.88	7
12	4	2.10	0.11	0.99	8.5
21	7	2.55	0.13	1.02	7

According to the experimental results reported by Kheder (1997), the primary cracks usually occur in the middle part of the wall followed by some inclined secondary cracks at corners. The

observed maximum crack widths usually occur at a height, h_{wm}, which is about 10% of the wall's length from the restraint edge. As it can be seen in figure 6.2, the simulated crack patterns are in reasonable agreement with these experimental results. In the non-linear simulations the maximum crack widths are in average located at a distance of about 8% of the wall's length from the restrained edge (see also table 6.1).
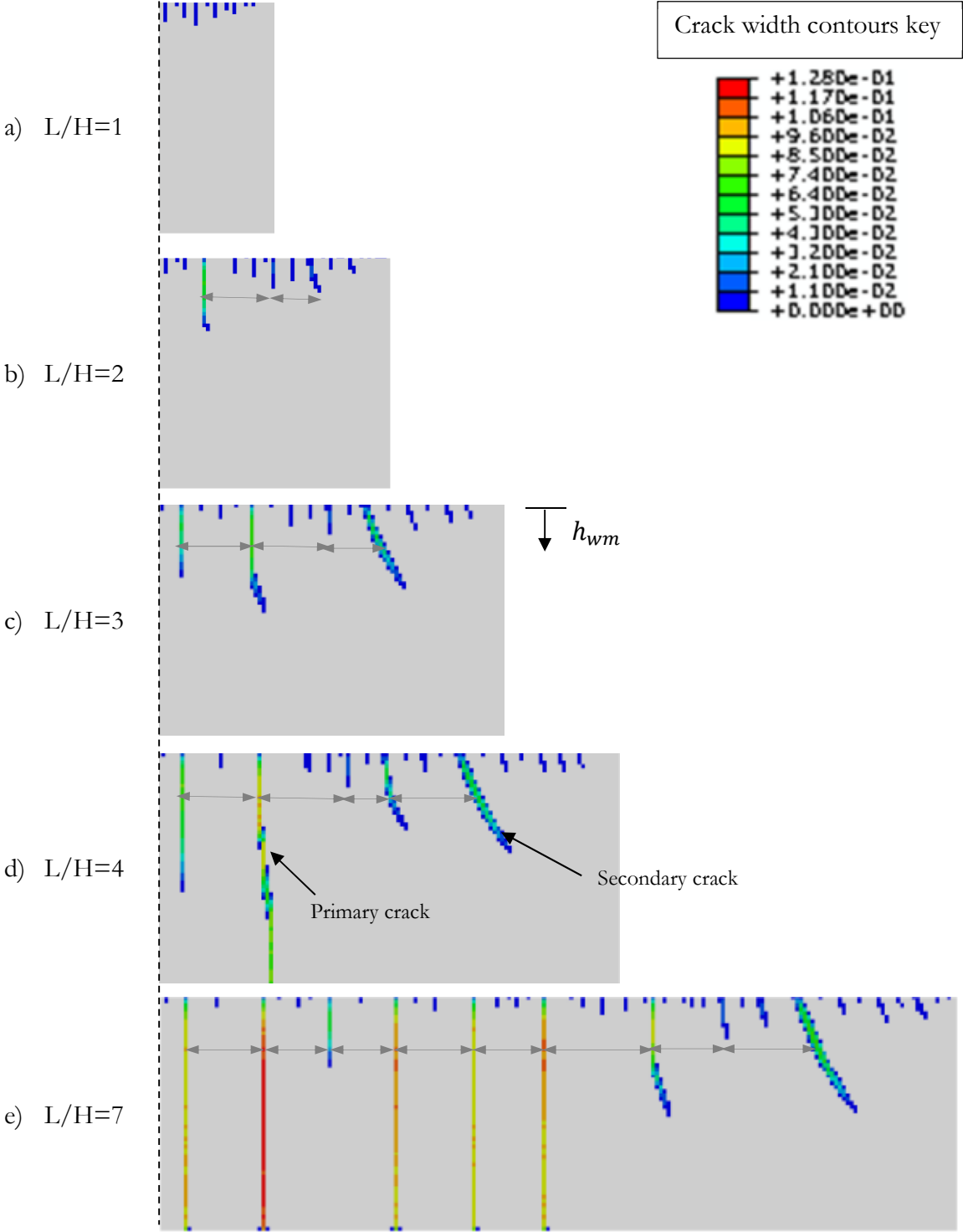

Figure 6.2 (a)-(e). Crack patterns in the transversal direction of the walls obtained by non-linear analysis

7. Discussion and Conclusions

7.1. Results and discussion

Figure 7.1 illustrates the comparison between maximum crack widths estimated by non-linear FE analyses and the EC2-3 approach for different L/H ratios. The results from both non-linear analysis and code calculations are obtained for test cases with a minimum reinforcement ratio (see also section 4.2). If the results of the non-linear analyses are taken as reference, it can be said that the crack width estimation method according to EC2-3 is on the safe side even for very high L/H ratios. However, the L/H ratios greater than 5 are rarely found in common slab frame bridge structures.
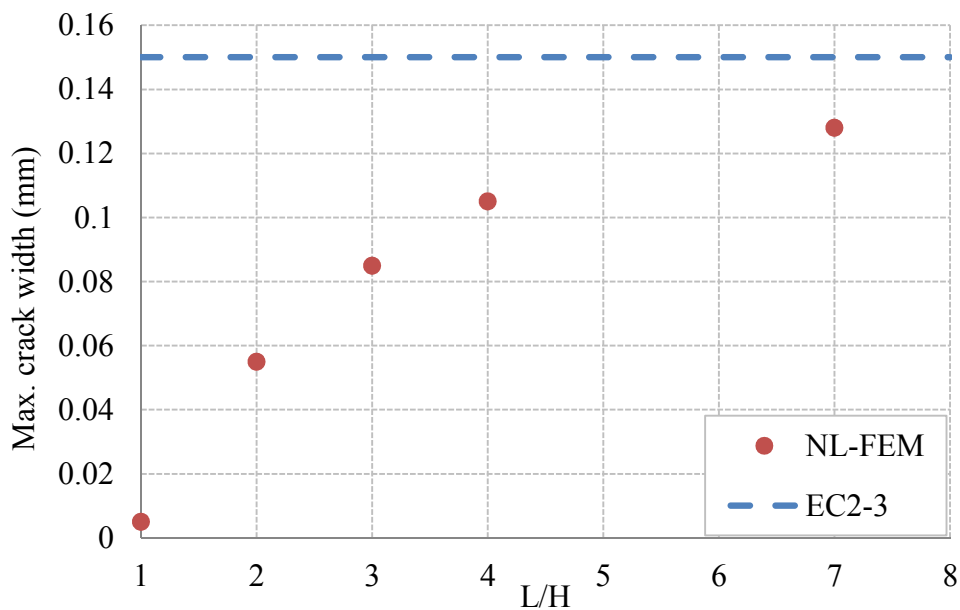

Figure 7.1. Comparison between estimated crack widths based on non-linear FEA and EC2-3 approach

Table 7.1 and figure 7.2 show the comparison between estimated crack width based on different approaches for a case study with L/H=4 for the minimum reinforcement ratio according to section 4.2. The results show that the crack widths estimated by the standard method in EC2-2 are much higher than for any of the other two methods. The reason is that the EC2-2 approach is suitable for external loading but for the case of restraint loading this method is not applicable. On the other hand, the EC2-3 approach is in rather good agreement with the result from the non-linear analyses and indicates that the EC2-3 approach is conservative.

Table 7.1. Comparison of estimated crack width based on different methods, for a case with L/H=4

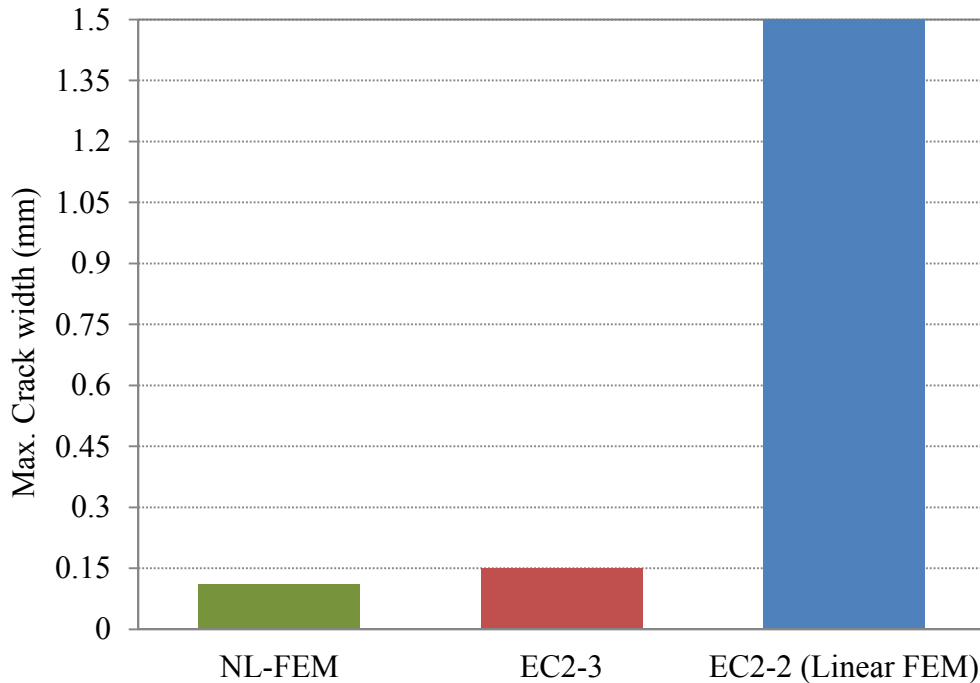| Approach	w_{max} (mm)
EC2-2 (Linear FE)	> 1.5[*]
EC2-3	0.15
Non-linear FE	0.11

[*] Reinforcing steel yields

Figure 7.2. Comparison of estimated crack width based on different methods for a case with L/H=4

Table 7.2 and figure 7.3 illustrate the comparison between the required reinforcement ratios according to different design approaches, i.e. EC2-2 and EC2-3, in order to limit the maximum crack width to values below 0.15mm. The results show that by using the EC2-3 approach, which is especially taylored for restraint loading, the required amount of reinforcement in the transversal direction of the wall was reduced to a very large extent.

As an example, for the case with L/H=4, the average reinforcement ratio over the height of the wall is reduced by a factor 10.

Table 7.2. Comparison between the required average reinforcement ratios
according to EC2-2 and EC2-3 for $w_{max} \leq 0.15mm$

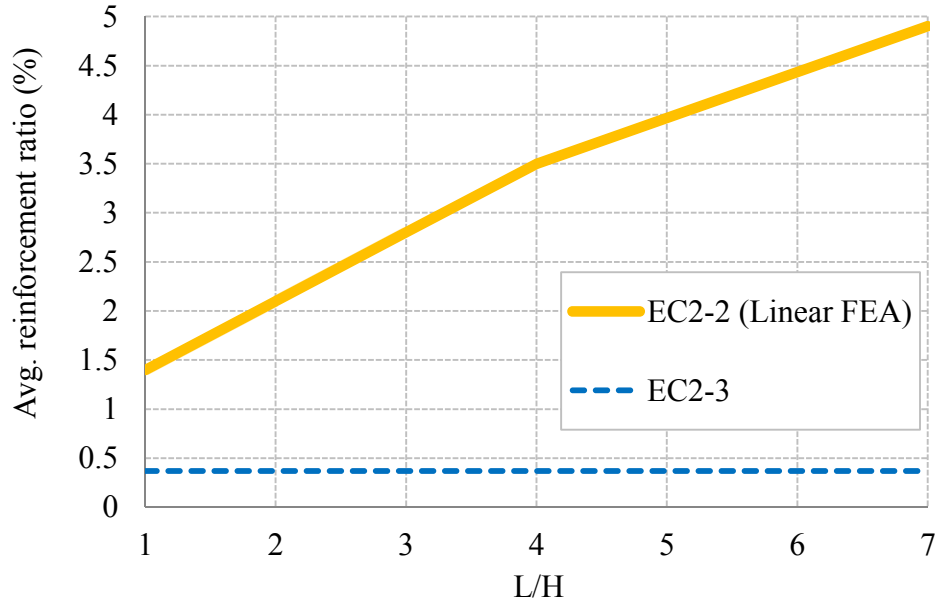| L (m)	L/H	EC2-2 (Linear FE)		EC2-3	
		ρ_s (%)	at each face	ρ_s (%)	at each face
3	1	1.4	$\phi 20 s 90 mm$		
6	2	2.1	$\phi 25 s 95 mm$		
9	3	2.8	$\phi 25 s 70 mm$	0.37^{*}	$\phi 12 s 125 mm$
12	4	3.7	$\phi 28 s 70 mm$		
21	7	4.9	$\phi 28 s 50 mm$		

* Minimum reinforcement ratio

34

Figure 7.3. Required average reinforcement ratios according to EC2-2 and EC2-3 for $w_{max} \leq 0.15mm$

In the EC2-3 approach a maximum crack distance $S_{r,max}$, according to equation (2.4) in section 2.4.3, is used to estimate the resulting crack width. However, in section 2.4.3 it is also stated that equation (2.4) may only be used in case stabilized cracking has been reached, and as mentioned in section 2.3 this rarely occurs in case of restraint loading. Consequently, to base the estimated crack width on a crack distance $S_{r,max}$ according to equation (2.4) may be on the unsafe side. Nevertheless, this approach is still recommended here based on the following reasons:

- The method is stated in EC2-3, and thereby supported by the standard.
- There will be other external loads that affect the stress state in the wall, e.g. ground pressure acting on the wing walls or effects caused by the poisons ratio, which will facilitate the forming of vertical cracks in the wall; and hence, make it easier for a stabilized crack state to be reached.
- According to Swedish experience there are no considerable problems with large vertical cracks in the walls of concrete slab frame bridges even though those to a large extent have been designed with a reinforcement amount that is smaller than that obtained by the method proposed in this report.

7.2.   Conclusions

A. The well-known standard procedure of crack width calculation in EC2-2 (2005) (see section 2.4.3) was determined for cases where stabilized cracking is reached under external loading. In the case of restraint loading, this approach in combination with results obtained from linear FE analysis is not applicable.
B. The recommended approach in EC2-3 (2006) (see section 2.4.4) can be used for calculation of crack widths in members restrained along one edge and subjected to thermal or shrinkage-imposed strains. Hence, this approach is suitable to crack control design in transversal direction of slab frame bridges subjected to thermal actions.
C. Both theoretical and experimental investigations show that the EC2-3 (2006) approach is conservative.
D. The results of nonlinear FE analysis show reasonable agreement with the estimated values based on the EC2-3 (2006) approach and indicated that the EC2-3 approach is conservative.

8. Recommendations

In design of concrete slab frame bridges with respect to crack width caused by restrained temperature/shrinkage strains in transversal direction, two approaches could be adopted in order to skip the effect of the very large restraint forces resulting from a linear FE analysis:

1. Relief the restrained forces in transversal direction by defining joint elements with very low transversal stiffness between the slab and the wall. The choice of this low stiffness is however rather arbitrary and such a procedure probably generates more problems than it solves.

2. For the transversal direction, ignore the effects of the temperature difference load case in the linear FE analysis. This amounts to defining two different load combinations one for the longitudinal and one for the transversal direction. Further, the ULS and SLS requirements in transversal direction of slab frame bridges under restrained thermal/shrinkage strains will be checked manually based on the recommendations in the EC2-3 (2006).

If alternative 2 is adopted a step by step design procedure is presented below:

Step by step design procedure:

A. Design the wall in the transversal direction for temperature/shrinkage

A1. Define the load cases

A1-1 Equivalent temperature difference due to shrinkage (ΔT_s):

According to EC2-1-1 (3.1.4, B.1 and B.2), the equivalent temperature difference due to the long-term total shrinkage strain should be calculated as

$$\Delta T_s = \frac{\varepsilon_{cs}}{\alpha_T (1 + \varphi_c)}$$

A1-2 Uniform temperature difference (ΔT_T):

According to EC1-1-5 (6.1.6), a uniform temperature difference equal to 15° should be applied between the main bridge structural parts (e.g. deck and wall or wall and foundation).

A2. Calculate the minimum reinforcement in sections subjected to tension

According to EC2-1-1 (7.3.2), a minimum amount of bonded reinforcement is required in order to control cracking in areas where tension is expected. The amount may be estimated from equilibrium between the tensile force in concrete just before cracking and the tensile force in reinforcement at yielding.

$$\rho_{s,\min} = \frac{k.k_c.f_{ctm}}{f_{yk}} \geq 0.2\%$$

For bridges, in order to take into account the effect of shrinkage the value of f_{ctm} used in evaluating the minimum reinforcement should be greater than 2.9MPa (see EC2-2 (7.3.2)).

A3. Define the maximum allowable crack width, w_{max}.

  According to EC2-2 (Table 7.101N), minimum concrete cover, c_{min}, and load factors for temperature/shrinkage in SLS load combination.

A4. Estimate the crack width in the wall due to shrinkage and temperature

  A4-1 Determine the total crack width due to temperature and shrinkage

  According to EC2-3 (M.3), in the case of a long wall restrained along one edge and subjected to thermal or shrinkage strains, if the minimum reinforcement is provided, the design crack width can be estimated as follows:

  $$w_k = S_{r,max}(\varepsilon_{sm} - \varepsilon_{cm})$$

  $$S_{r,max} = 7\phi + \frac{0.425 k_1 k_2 \phi}{\rho_{eff}} \qquad (EC2 - 1 - 1 : eq.\,7.11)$$

  $$\varepsilon_{sm} - \varepsilon_{cm} = R\,(\alpha_T.\Delta T)$$

  where R is the restraint factor taking into account the effect of the edge. According to table L.1, the maximum restraint degree is equal to R=0.5. The total crack width due to temperature/shrinkage (w_{TS}) then becomes:

  $$w_{TS} = w_T + w_S$$

  A4-2 Define the cracked regions due to edge restraint shrinkage/temperature strains

  The results of experimental investigations on base restraint walls subjected to temperature/shrinkage strains published by Kheder (1997) indicate that the primary cracks typically occur in the middle of the wall followed by some inclined cracks at corners and there are areas close to the side edges of the wall which remain un-cracked, see figure 8.1.
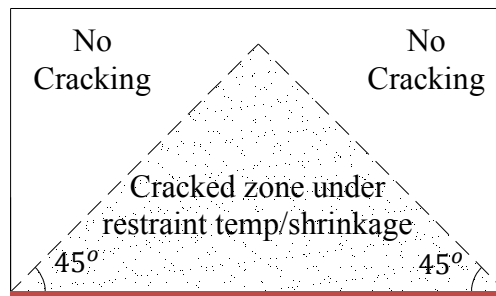

Figure 8.1. Area where cracking from restrain temperature loading occurs

B. Design the extra reinforcements due to the effects of other load cases

B1. Define different limits for allowable crack width in different regions of a frame wall (a) or a bridge deck (b) with edge restraints at both edges as shown in figure 8.2.

bridge deck

$$w_{max,n} = w_{max} - w_{TS}$$

w_{max} w_{max}

$$w_{max,n} = w_{max} - w_{TS}$$

bottom plate

(a)

wall

$$w_{max,n} = w_{max} - w_{TS}$$

w_{max}

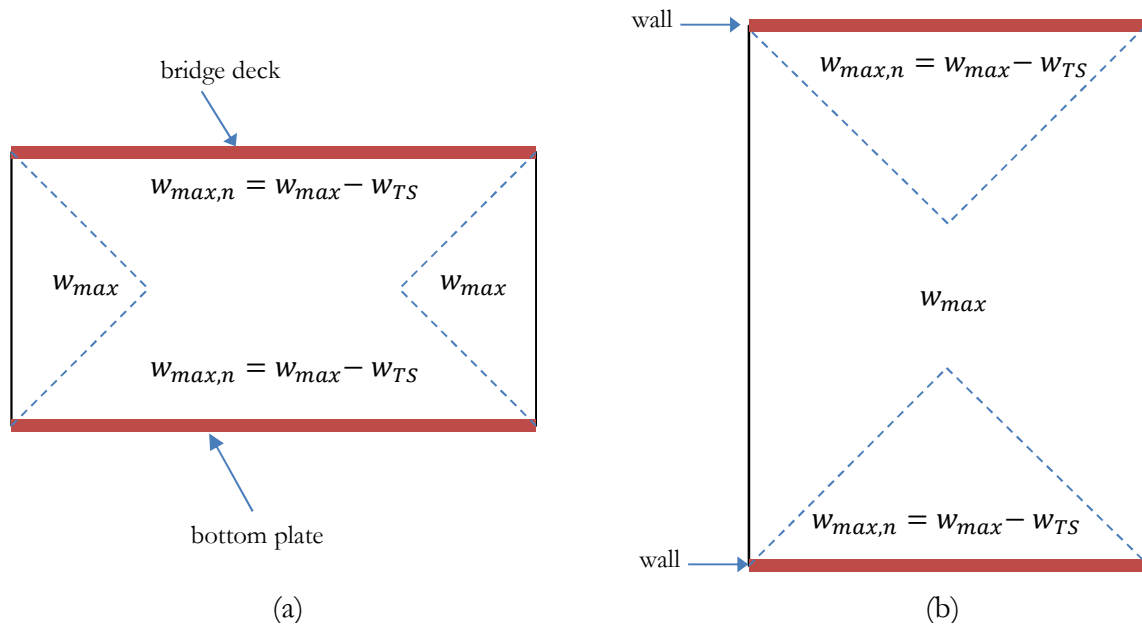$$w_{max,n} = w_{max} - w_{TS}$$

wall

(b)

Figure 8.2. Different regions for crack width limits in (a) a wall restrained by the bridge deck and the bottom plate (b) a bridge deck restrained by the walls

B2. Design the wall or the bridge deck based on the envelope of ULS and SLS load combinations for all related load cases excluding temperature and shrinkage

Bibliography

1. ACI, 1995, Effect of restraint, volume change and reinforcement on cracking of mass concrete, ACI207.2R, ACI Manual of concrete practice, Part 1, American concrete institute, USA
2. Alfredsson H., Spåls J., 2008, Cracking behavior of Concrete Subjected to Restraint Forces. Master's Thesis 2008:24. Division of Structural Engineering, Chalmers University of Technology, Göteborg, Sweden.
3. Andersson J., Andersson L., 2010., Tvångskrafter i betongbroar, Analys och implementering av metod för reducering av tvångskrafter, Master thesis, Lund University, Sweden (In Swedish)
4. Antona B., Johansson R., 2011, Crack Control of Concrete Structures Subjected to Restraint Forces. Master's Thesis 2011:70, Division of Structural Engineering, Chalmers University of Technology, Göteborg, Sweden.
5. Bamforth P., 2007, Early-age thermal crack control in concrete, CIRIA Report C660
6. Bamforth P.,Denton S., Shave J., 2010, The development of a revised unified approach for the design of reinforcement to control cracking in concrete resulting from restrained contraction, ICE Research project 0706
7. Cope R.J., Clark L.A., Concrete slabs - Analysis and design, London 1984, ISBN: 0-85334 254-7
8. EC2-1-1, 2004. Eurocode 2: Design of concrete structures Part 1-1: General Common rules for building and civil engineering structures
9. EC1-1-5, 2003. Eurocode 1: Actions on structures Part 1-5: General actions – Thermal actions
10. EC2-2, 2005. Eurocode 2: Design of concrete structures Part 2: Concrete bridges – Design and detailing rules
11. EC2-3, 2006. Eurocode 2: Design of concrete structures Part 3: Liquid retaining and containment structures
12. Engström B., (2011): Restraint cracking of reinforced concrete structures. Division of Structural Engineering, Chalmers University of Technology, Göteborg, Sweden, 2008.
13. Ghali A., Favre R., Elbadry M. (2002): Concrete Structures, Stresses and Deformations, Third Edition. Spon Press, London, Great Britain, 2002, 473 pp.
14. Hibbitt, Karlsson, Sorensen, 2011, Abaqus User's Manual, Pawtucket, 6th Edition
15. Johansson P., Lantz H., 2009, Crack Control of Reinforced Concrete with Continuous Edge Restraint. Master's Thesis 2009:43. Division of Structural Engineering, Chalmers University of Technology, Goteborg, Sweden.
16. Kheder G.F., 1997, A New Look at the Control of Volume Change Cracking of Base Restrained Concrete Walls, ACI Structural Journal, May-June 1997, pp. 262-271
17. Pettersson D., Thelandersson S., 2001, Crack development in concrete structures due to imposed strains - Part I: Modelling, Materials and Structures, Vol. 34, Jan-Feb 2001, pp. 7-13
18. MC2010, 2010. CEB-FIP Model Code 2010, Design Code, 1st draft, Thomas Telford, Lausanne, Switzerland.
19. Svensk byggtjänst, 1994, Betonghandbok Material (Concrete handbook Material), Chapter 16, pp. 547-607, Sweden.

Appendix A: Mesh Convergence study

Table A.1 presents the results of the mesh convergence study for a wall with 10m length and 4.5m height subjected to a temperature drop equal to $\Delta T=15^{\circ}$. Both vertical and horizontal reinforcement ratios are about 0.2%. The non-linear analyses have been performed for 4 different mesh sizes. According to the results in the table an element size smaller than 2 cm should be chosen.

Table A.1. Results of mesh convergence study for a 10x4.5 m^2 wall (ρ=0.2%)

l_e (cm)	$\sigma_{s,max}$ (MPa)	$\varepsilon_{x.max}$ $\times 10^{-3}$	$w_{k,max}$ (mm)
10	300	1.721	0.172
5	273	2.612	0.131
2	254	5.146	0.103
1	247	9.914	0.099

The crack patterns obtained from FE models with different mesh sizes are shown in Figure A.1. As it can be shown in this figure, for models with element sizes smaller than 2cm both the crack patterns and estimated maximum crack widths are approximately similar.
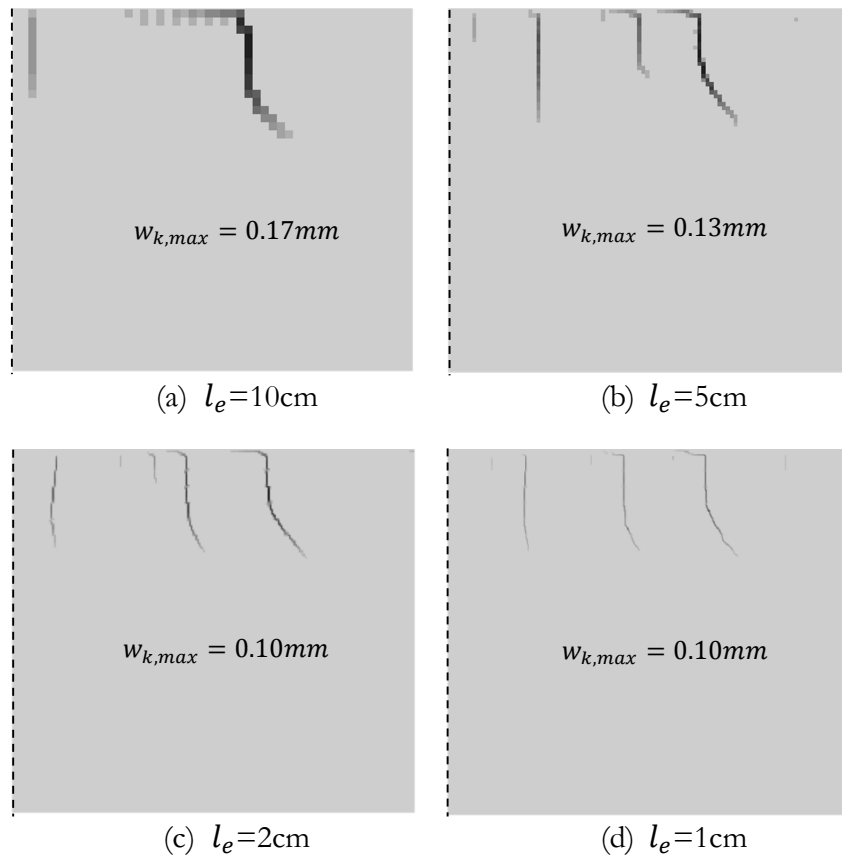

$w_{k,max} = 0.17mm$

(a) l_e=10cm

$w_{k,max} = 0.13mm$

(b) l_e=5cm

$w_{k,max} = 0.10mm$

(c) l_e=2cm

$w_{k,max} = 0.10mm$

(d) l_e=1cm

Figure A.1. Crack patterns obtained based on different mesh sizes for 10x4.5m^2

However, using such a small element size ($2x2cm^2$) for all test cases is extremely time-consuming. For this reason, the FE-models used in the analyses have been discretized with 5 by 5 cm elements. In this way, the obtained crack widths are slightly over estimated. It should be noted

that in the mesh convergence study, the non-linear analysis has been performed by using the concrete damage plasticity material model instead of the smeared cracking model.

Appendix B: Uniaxial response curves of material models

In this appendix the uniaxial response curves of material models which were used in the non-linear analysis are presented.

Thus, figure B.1 shows the bilinear tensile stress-cracking strain diagram for the uniaxial tensile behavior of concrete according to MC2010 (2010). The pre-peak stress-strain diagram for concrete in uniaxial compression according to EC2-1-1 (2004) is illustrated in figure B.2. Figure B.3 presents the bilinear elastic-perfectly plastic stress-strain diagram used for modeling the nonlinear behavior of reinforcing steel based on EC2-1-1 (2004). The input values for defining the curve data can be found in table 3.1 as basic material properties.
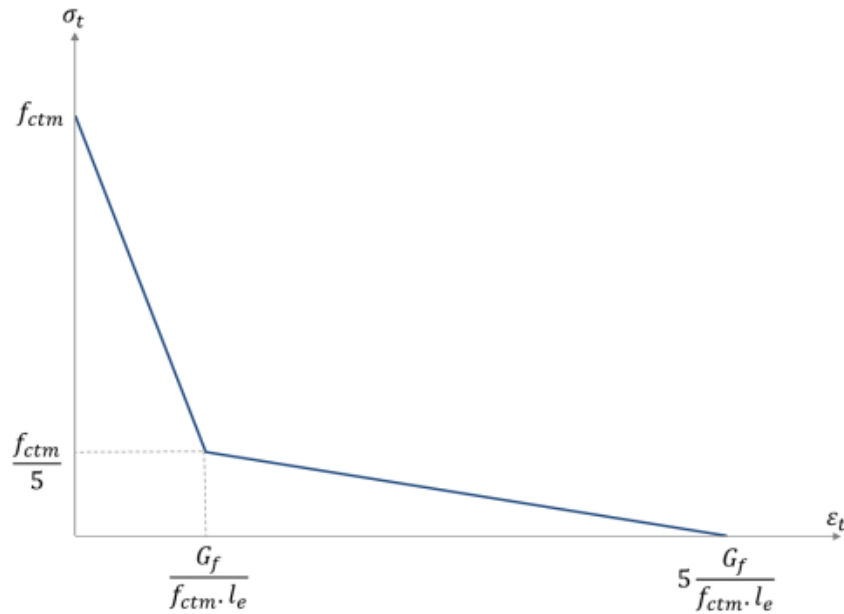

Figure B.1. Bilinear stress-cracking strain diagram for concrete in uniaxial tension (MC2010, 2010)
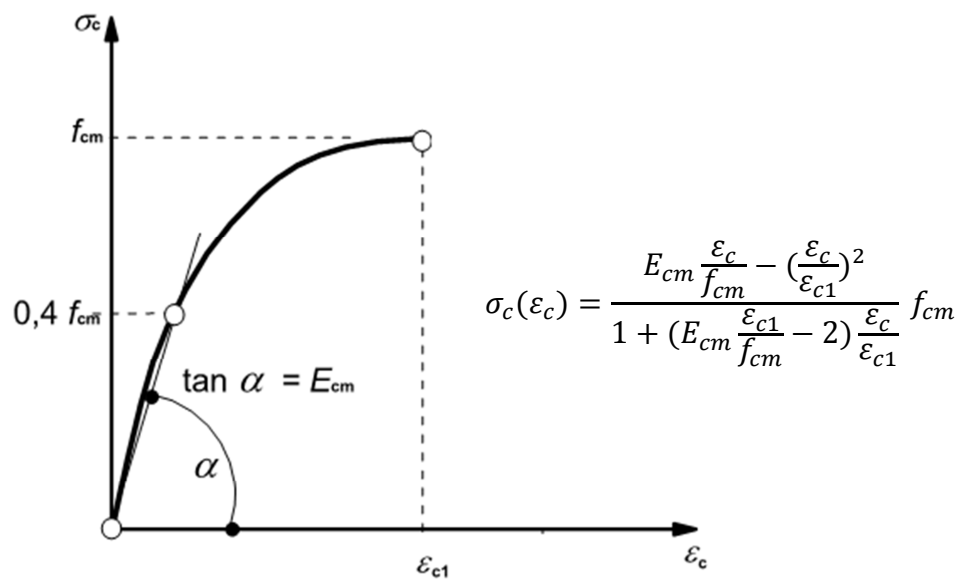

$$\sigma_c(\varepsilon_c) = \frac{E_{cm}\frac{\varepsilon_c}{f_{cm}} - (\frac{\varepsilon_c}{\varepsilon_{c1}})^2}{1 + (E_{cm}\frac{\varepsilon_{c1}}{f_{cm}} - 2)\frac{\varepsilon_c}{\varepsilon_{c1}}} f_{cm}$$

Figure B.2. Pre-peak stress-strain diagram for concrete in uniaxial compression (EC2-1-1, 2004)
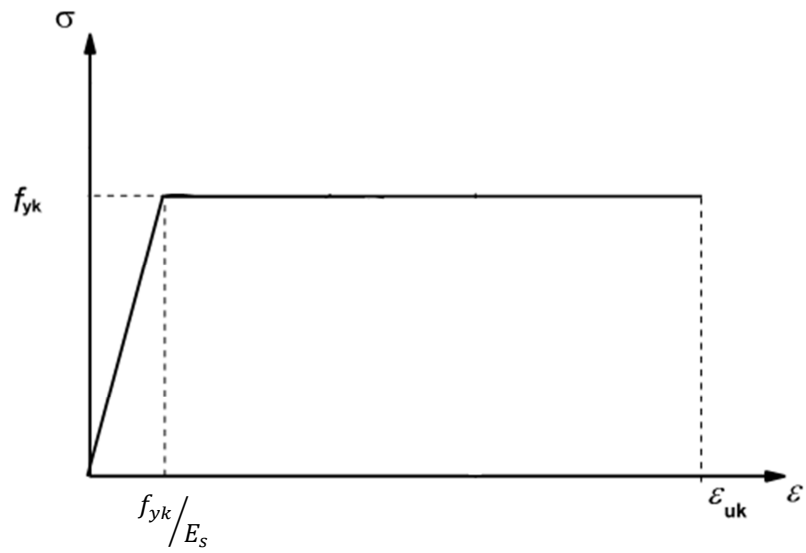
Figure B.3. Bilinear elastic-perfectly plastic stress-strain diagram for steel (EC2-1-1, 2004)